[5] R. Paknys and N. Wang, "Creeping wave propagation constants and modal impedance for a dielectric coated cylinder," *IEEE Trans. Antennas Propagat.*, vol. AP-34, pp. 674–680, May 1986.
[6] ——, "Excitation of creeping waves on a circular cylinder with a thick dielectric coating," *IEEE Trans. Antennas Propagat.*, vol. AP-35, pp. 1487–1489, Dec. 1987.
[7] E. J. Rothwell and M. J. Cloud, *Electromagnetics*. Boca Raton, FL: CRC Press, 2001.
[8] C. A. Balanis, *Advanced Engineering Electromagnetics*. New York: Wiley, 1989.

High-Order Symplectic Integration Methods for Finite Element Solutions to Time Dependent Maxwell Equations

R. Rieben, D. White, and G. Rodrigue

***Abstract*—In this paper, we motivate the use of high-order integration methods for finite element solutions of the time dependent Maxwell equations. In particular, we present a symplectic algorithm for the integration of the coupled first-order Maxwell equations for computing the time dependent electric and magnetic fields. Symplectic methods have the benefit of conserving total electromagnetic field energy and are, therefore, preferred over dissipative methods (such as traditional Runge–Kutta) in applications that require high-accuracy and energy conservation over long periods of time integration. We show that in the context of symplectic methods, several popular schemes can be elegantly cast in a single algorithm. We conclude with some numerical examples which demonstrate the superior performance of high-order time integration methods.**

***Index Terms*—Finite element methods, high-order methods, Maxwell equations, symplectic methods, time domain analysis.**

I. Introduction

We are concerned with the finite element solution of the time dependent Maxwell equations on unstructured grids using a combination of both high-order spatial and high-order temporal discretization methods. In this paper we focus our attention on the high-order temporal discretization process, and we investigate the use of symplectic integration methods. Such methods were originally developed to solve numerical systems derived from a Hamiltonian formulation and have been successfully used in the fields of astronomy and molecular dynamics where numerical accuracy and energy conservation are very important over large time integration periods [1]. Recently, these methods have been adapted for use in computational electromagnetics (CEM) in conjunction with the finite difference method. In [2] and [3] a symplectic finite-difference time-domain (FDTD) algorithm is presented that is implicit, fourth order accurate and valid for orthogonal three-dimensional grids . In [4] and [5], the authors present a modified symplectic FDTD method that is up to fourth-order accurate in space and time. A variation using the linear "serendipity" finite elements of [6] is also mentioned. Here, we proceed in a similar manner using high-order symplectic integration methods in conjunction with a high-order vector finite element method for use in nonorthogonal, unstructured grids. The spatial discretization is handled by the use of Nédeléc [7] basis functions of *arbitrary* order which are based on the properties of differential forms [8], [9]. For the Galerkin procedure applied to either the frequency domain or time dependent Maxwell equations [10], there are significant advantages to both one-form and two-form finite element basis functions [11]; including the proper modeling of the jump discontinuity of field intensities and flux densities across material interfaces, the elimination of spurious modes in eigenvalue computations and the conservation of charge in time-dependent simulations [11]. These properties are crucial for the elimination of late time instabilities caused by improper spatial discretization as investigated by [12]–[14].

We begin with a method of lines approach to the discretization of the time dependent Maxwell equations. We approximate the coupled partial differential equations using a high-order vector finite element scheme which yields a linear system of ordinary differential equations (ODEs). This system is then be discretized in time via a finite difference method to produce a series of update steps which propagate the solutions forward in time. However, most high-order numerical integration methods (e.g., Runge–Kutta, Adams–Bashforth) are dissipative. This can lead to misleading results for systems that need to be iterated for long time intervals [15], [16]. A solution is to use a symplectic time integration method that conserves energy. Therefore, in this paper we investigate and promote the use of symplectic methods for the time integration of Maxwell's equations.

II. Ampere-Faraday System

We begin with the coupled first-order time dependent Maxwell equations

$$\epsilon \frac{\partial}{\partial t}\mathbf{E} = \nabla \times (\mu^{-1}\mathbf{B}) - \mathbf{J}(t)$$
$$\frac{\partial}{\partial t}\mathbf{B} = -\nabla \times \mathbf{E} \tag{1}$$

where ϵ and μ are (possibly tensor valued) functions representing the material properties of the system and $\mathbf{J}(t)$ is a time dependent current source. Using a Galerkin finite element procedure with one-form (or $Curl$-conforming) vector basis functions to discretize the electric field intensity and two-form (or Div-conforming) vector basis functions to discretize the magnetic flux density yields the following linear system of ODEs

$$A\ \frac{\partial}{\partial t} e = K^T D\ b - A\ j$$
$$\frac{\partial}{\partial t} b = -K\ e \tag{2}$$

where e and b represent the discrete differential one-form and two-form electric and magnetic fields, respectively, K represents the discrete $Curl$ operator (i.e., the topological derivative matrix), A is the one-form mass matrix computed using the material property function ϵ to represent the dielectric properties, D is the two-form mass matrix computed using the material property function μ^{-1} to represent the magnetic permeability and j is the discrete two-form time dependent current source. Note that the vectors e and b will have different dimensions and that the matrix K will be rectangular. This is due to the dimensions of the Nédeléc polynomial spaces from which they are

Manuscript received April 23, 2003; revised September 22, 2003. This work was performed under the auspices of the U.S. Department of Energy by the University of California, Lawrence Livermore National Laboratory under contract W-7405-Eng-48 and the U.S. Air Force under Contract F49620-01-1-0327.

R. Rieben and G. Rodrigue are with the University of California Davis and Institute for Scientific Computing Research, Lawrence Livermore National Laboratory, Livermore, CA 94551 USA (e-mail: rieben1@llnl.gov; ghrodrigue@ucdavis.edu).

D. White was with the Center for Applied Scientific Computing Research, Lawrence Livermore National Laboratory, Livermore, CA 94551 USA (e-mail: white37@llnl.gov). He is now with the Defense Sciences Engineering Division, Lawrence Livermore National Laboratory, Livermore CA, 94551 USA (e-mail: white37@llnl.gov).

Digital Object Identifier 10.1109/TAP.2004.832356

derived [7]. For an electromagnetic problem with no physical dissipation due to conductivity or absorbing boundary conditions the total electromagnetic energy should remain constant. In this particular finite element method the instantaneous energy is the numerical version of the total energy given by

$$\mathcal{E} = e^T A\, e + b^T D\, b. \tag{3}$$

Many time integration methods such a forward Euler, backward Euler, Runge–Kutta, Adams–Bashforth, etc. are inherently dissipative and the energy as measured by (3) is not conserved; given an initial condition the electromagnetic energy will decay exponentially.

The very popular second-order central difference (also known as a "leap frog") method applied to system (2) can be written as

$$\begin{aligned} e_n &= e_{n-1} + \Delta t(A^{-1}K^T D\, b_{n-1/2} - j) \\ b_{n+1/2} &= b_{n-1/2} + \Delta t(-K\, e_n). \end{aligned} \tag{4}$$

It is well known that this particular method is both conditionally stable and nondissipative; the energy as measured by (3) is conserved. Our goal is to apply higher order energy conserving time integration methods to system (2). This is required to take full advantage of the higher order finite element basis functions. The resulting method is higher order in both space and time and will have significantly less numerical dispersion than low-order FDTD type methods, which is important for electrically large problems.

III. Conservative Time Integration

Consider a general system of ODEs, with field values p and q and an independent variable t, that is of the specific form

$$\begin{aligned} \frac{\partial}{\partial t} p &= F(q,t) \\ \frac{\partial}{\partial t} q &= G(p). \end{aligned} \tag{5}$$

Systems of this form have the property of being nondissipative, i.e., the system does not lose energy as it evolves in time. Numerical integration methods for solving system (5) should likewise be nondissipative. For linear equations, such methods are typically written as an update scheme of the form

$$\begin{bmatrix} p_{n+1} \\ q_{n+1} \end{bmatrix} = \mathbf{M} \begin{bmatrix} p_n \\ q_n \end{bmatrix} \tag{6}$$

where the field values at a new state are expressed in terms of values at previous states. There are three specific cases of interest based on the matrix norm of $\mathbf{M}$, given by

$$|\mathbf{M}| \begin{cases} > 1, & \text{unstable} \\ = 1, & \text{neutrally stable (nondissipative)} \\ < 1, & \text{stable, dissipative.} \end{cases} \tag{7}$$

When the eigenvalues of the update matrix all lie within the unit circle in the complex plane, the method will be stable and dissipative. Nondissipative methods have the additional property that the eigenvalues of the update matrix all lie *on* the unit circle in the complex plane, with additional constraints on the eignevectors for stability [11]. The mapping is said to be symplectic if the following relation holds [17]

$$\partial\mathbf{M}^T\, \mathbf{S}\, \partial\mathbf{M} = \mathbf{S} \tag{8}$$

where

$$\partial\mathbf{M} = \begin{bmatrix} \partial_p \tilde{F} & \partial_q \tilde{F} \\ \partial_p \tilde{G} & \partial_q \tilde{G} \end{bmatrix}; \quad \mathbf{S} = \begin{bmatrix} 0 & \mathbf{I} \\ -\mathbf{I} & 0 \end{bmatrix}$$

TABLE I
Coefficients for Methods of Order One Through Four

Order 1 – Truncation Error = Δt^2	
$a_1 = 1$	$b_1 = 1$
Order 2 – Truncation Error = Δt^3	
$a_1 = 1/2$	$b_1 = 0$
$a_2 = 1/2$	$b_2 = 1$
Order 3 – Truncation Error = Δt^4	
$a_1 = 2/3$	$b_1 = 7/24$
$a_2 = -2/3$	$b_2 = 3/4$
$a_3 = 1$	$b_3 = -1/24$
Order 4 – Truncation Error = Δt^5	
$a_1 = (2+2^{1/3}+2^{-1/3})/6$	$b_1 = 0$
$a_2 = (1-2^{1/3}-2^{-1/3})/6$	$b_2 = 1/(2-2^{1/3})$
$a_3 = (1-2^{1/3}-2^{-1/3})/6$	$b_3 = 1/(1-2^{2/3})$
$a_4 = (2+2^{1/3}+2^{-1/3})/6$	$b_4 = 1/(2-2^{1/3})$

where $\tilde{F}$ and $\tilde{G}$ represent discretized versions of the original functions F and G. The matrix $\mathbf{S}$ is referred to as the *symplectic matrix*, where the word symplectic literally means "intertwined." Note that this definition only makes sense if the vectors of unknowns p and q are of the same dimension, as in the case of a Hamiltonian system where q denotes the generalized coordinates and p the generalized momenta.

As a specific example, consider the simple harmonic oscillator (SHO) where $F(q,t) = q$ and $G(p) = -p$. An exact solution to this simple problem is given by $p(t) = \sin(t)$ and $q(t) = \cos(t)$. We can quantify the energy of this system (i.e., a *conserved* or constant quantity) by the value

$$\mathcal{E} = p^2(t) + q^2(t)$$

which for this specific example is equal to 1. Applying the leap frog method to the SHO yields the following update scheme

$$\begin{bmatrix} p_n \\ q_{n+1/2} \end{bmatrix} = \begin{bmatrix} 1 & \Delta t \\ -\Delta t & (1-\Delta t^2) \end{bmatrix} \begin{bmatrix} p_{n-1} \\ q_{n-1/2} \end{bmatrix}.$$

It is a straightforward calculation to show that this update scheme satisfies (8) and is therefore symplectic. However, it is also straightforward to show that this mapping does not conserve the exact value of $\mathcal{E}$ under iteration. This is due to the fact that symplectic maps solve *some* Hamiltonian exactly, but not the exact one of the system [1], [17]. However, as shown by Yoshida [18], the numerical value of the inexact conserved quantity $\tilde{\mathcal{E}}$ oscillates about the exact value $\mathcal{E}$ and the amplitude of this oscillation is reduced as the order of the symplectic method is increased.

To demonstrate the properties of symplectic integrators for conservative systems, we proceed to solve the SHO system numerically using both a symplectic method (the order three case from Table I) and a nonsymplectic fourth-order Runge–Kutta method. In both cases, the system is propagated from $t = 0$ to $t = 250$ using a time step of $\Delta t = 0.8$ and the computed maximum global phase error will grow linearly at each time step. Where the two cases differ is in the computation of the energy of the system. Fig. 1 shows the computed numerical energy of the system at each time step for both methods. For the symplectic method, the numerical energy is of the form

$$\tilde{\mathcal{E}} = \delta_1 \cos(\gamma_1\, t)\, \mathcal{E}$$

while for the nonsymplectic method the energy is of the form

$$\tilde{\mathcal{E}} = \delta_2 \exp(-\gamma_2\, t)\, \mathcal{E}.$$

Fig. 2 shows a parametric plot of the conjugate variables as a function of time. The numerical energy for the symplectic method oscillates at a fixed amplitude around the exact value, and is therefore conserved (in

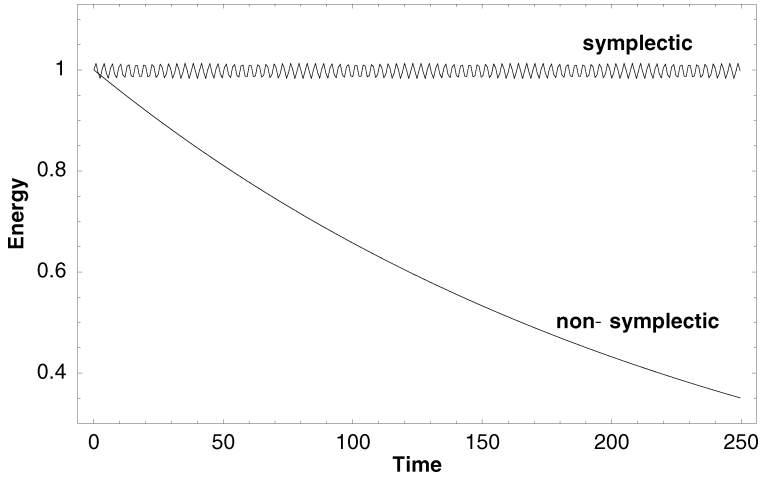

Fig. 1. Numerical energy at each time step using a symplectic method and a nonsymplectic Runge–Kutta method.

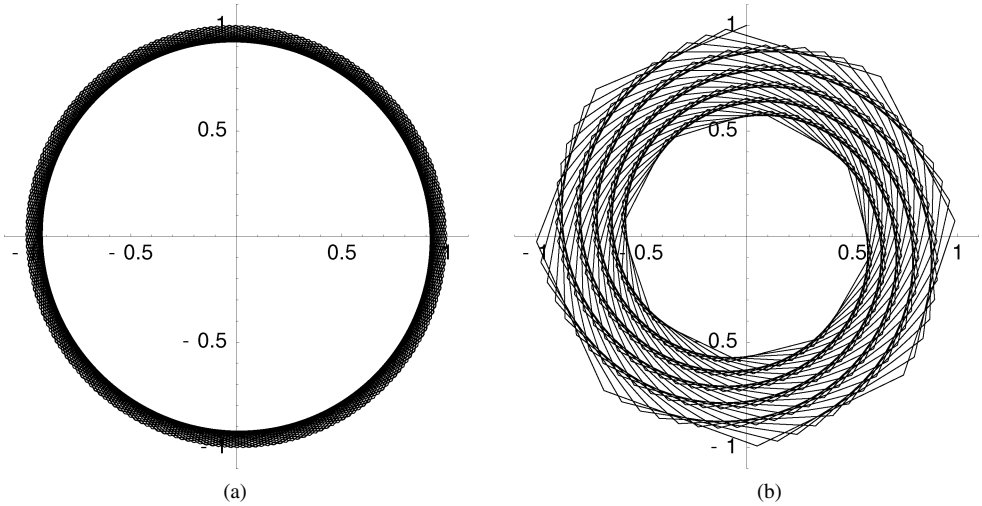

(a) (b)

Fig. 2. Parametric phase plots of the conjugate variables of a simple harmonic oscillator using (a) a symplectic method and (b) a nonsymplectic Runge–Kutta method.

a time averaged sense). The energy for the nonsymplectic method dissipates exponentially from the exact value, indicating spurious dampening of the system.

Such behavior is typical of symplectic methods when applied to conservative systems, and has therefore motivated us to apply them to the particular system of (2). It should be noted that when a symplectic method is applied to the Maxwell system of ODEs (2) the result does not satisfy the symplectic property of (8). This is due to the fact (as mentioned previously) that the vectors e and b are not of the same dimension and that the matrix K is rectangular. Nevertheless this does not preclude the method from being used, in fact it has been successfully used in FDTD schemes where the dimension of e (the number of mesh edges) is different than the dimension of b (the number of mesh faces) [2], [3]. We demonstrate through computational experiments in Section V that high-order symplectic methods do work when applied to system (2) and correctly reproduce the previously mentioned features of stability, high accuracy, and no nonphysical dissipation.

IV. General Symplectic Algorithm

We now present the general symplectic integration algorithm used in our experiments. The algorithm is valid for ODE systems of the form (5), such as (2). The inputs, procedure and outputs of the method are presented in Algorithm 1. Numerical methods for the integration of a set of differential equations are typically characterized by the accuracy of a single step in time (the independent variable). If for some small time step Δt the integration is performed so that it is accurate through order Δt^k, then the method is of kth order. In general, a method of order k will require k evaluations of the functions F and G. Therefore, as the order of the method is increased the overall computational costs will increase likewise. However, as we will show in the next section, for higher order methods, it is possible to increase the size of the time step Δt (while still maintaining numerical stability), thereby reducing the overall number of time steps. The order of the method can be adjusted simply by providing the algorithm with a corresponding set of coefficients, a and b, each of length $order$. Table I lists exact values of the sets of coefficients a and b for methods of order one through four, as originally computed by Ruth [15] and Candy [19].

Algorithm 1: General Symplectic Integration Algorithm
input : $order$, the order of the method $F(q,t)$ and $G(p)$, two functions a and b, two sets of coefficients F_0 and G_0, the initial conditions t_0 and t_{fin}, initial and final time Δt, the time step to use
output : p_{fin} and q_{fin}, the fields at time t_{fin}

Compute the number of time steps:

$$nstep = \frac{t_{\text{fin}} - t_0}{\Delta t}$$

Set initial conditions:

$$p_1 \leftarrow F_0$$
$$q_1 \leftarrow G_0$$

Begin loop over time steps:
for $i = 1$ ***to*** $nstep$ **do**

Begin integration method update :
$p_{\text{in}} \leftarrow p_i$
$q_{\text{in}} \leftarrow q_i$
for $j = 1$ ***to*** $order$ **do**
Compute the update time for this step :
$t_j = i * \Delta t + \sum_{k=1}^{j-1} a_k * \Delta t$
Update the field values :
$p_{\text{out}} = p_{\text{in}} + b_j * \Delta t * F(q_{\text{in}}, t_j)$
$q_{\text{out}} = q_{\text{in}} + a_j * \Delta t * G(p_{\text{out}})$
$p_{\text{in}} \leftarrow p_{\text{out}}$
$q_{\text{in}} \leftarrow q_{\text{out}}$
end
Update field values for this time step :
$p_{i+1} \leftarrow p_{\text{out}}$
$q_{i+1} \leftarrow q_{\text{out}}$

end
$p_{\text{fin}} \leftarrow p_{nstep+1}$
$q_{\text{fin}} \leftarrow q_{nstep+1}$

V. Numerical Examples

We now present some computational examples using the symplectic integration algorithm in conjunction with high-order finite element matrices for the spatial discretization of Maxwell's equations. The computational domain for these examples is a unit cube subject to either a PEC (Dirichlet) or a natural zero flux (Neumann) boundary condition. The Ampere-Faraday system is discretized in space using a very coarse eight element hexahedral mesh in conjunction with high-order vector basis functions of polynomial degree $p = 4$

In each of the following examples, the time integration schemes are subject to a stability condition. This stability condition is based on the spectral radius of the amplification matrix which is applied to the system at every time step in an update method of the form (6). For the discrete Maxwell equations of system (4), there exists an upper bound on the largest stable time step given by [11]

$$\Delta t \leq \frac{2}{\sqrt{MaxEig(A^{-1}K^T DK)}}. \tag{9}$$

We have found that about 0.95 times the upper bound of this constraint is sufficient for symplectic methods of order one through three; higher order methods require a smaller time step to remain stable. For example, we have found that for the fourth-order method from Table I, about 0.70 times the upper bound is sufficient for stability.

In addition, for each of the following examples, evaluation of the function F during the update phase requires that a linear system involving the matrix A must be solved. To simplify this process, we perform the linear solve using a diagonally scaled Conjugate Gradient algorithm. However, this process could be made more efficient by using a sparse direct solver.

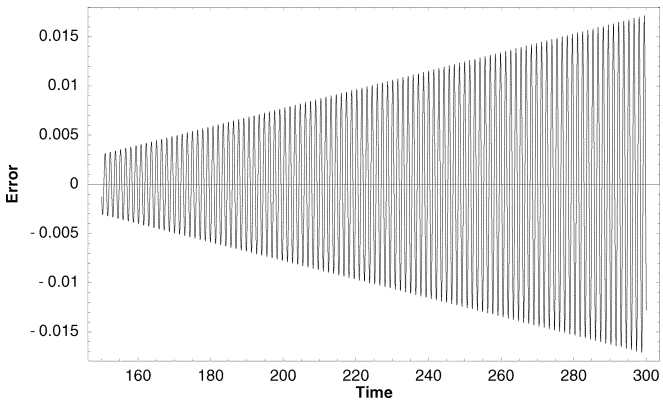

Fig. 3. Global phase error at each time step for the first-order symplectic integration method.

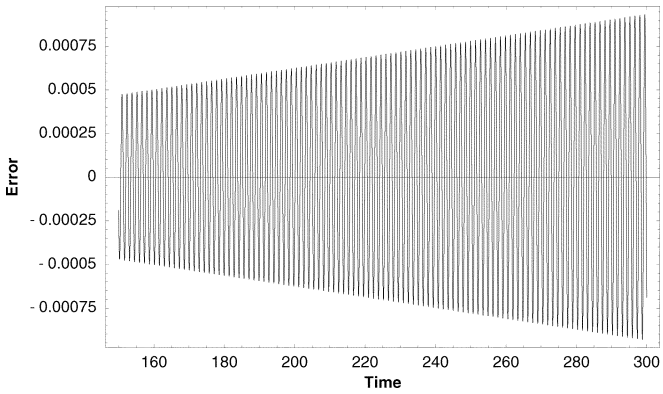

Fig. 4. Global phase error at each time step for the third-order symplectic integration method.

A. Example 1

In this example we demonstrate the growth of global phase error for the time integration of (2) using two different methods. We begin by solving the general eigenvalue problem

$$Sx = \lambda Ax \tag{10}$$

subject to a zero flux boundary condition [20]. Here, S is the one-form stiffness matrix (i.e the $Curl-Curl$ matrix) and this system represents the resonant modes of the unit cube. We locate the first nonzero eigenvalue of this system (representing the first resonant mode of the cavity) and its corresponding eigenvector. Using basis functions of polynomial degree $p = 4$ on a coarse eight element mesh, the first resonant mode is computed to an accuracy of 10^{-4}. We then use the computed eigenvector as the initial condition for the electric field in (2), the magnetic field will have a zero value initial condition. System (2) is then propagated forward in time for a total of 300 s (using a value of unity for the speed of light). The resulting computed electric field will be an oscillatory cosine wave with a frequency equal to the first resonant mode of the cube. We compare the global phase error in the computed solution against the exact value using both a first and third-order symplectic integration method. The first-order method is integrated using a time step of $\Delta t = 0.005$ s yielding a total of 60,000 time steps while the third-order method is integrated using a time step of $\Delta t = 0.015$ s yielding a total of 20 000 time steps. The resulting computations therefore require the same total amount of CPU time to complete. The resulting global phase errors are shown in Figs. 3 and 4. Note that in both cases, the maximum global phase error grows linearly at each time step, but the third-order method yields a much slower rate of growth with a

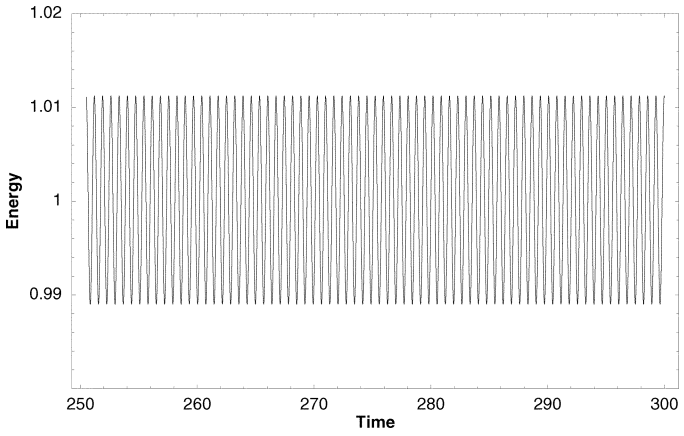

Fig. 5. Numerical energy at each time step for the first-order method.

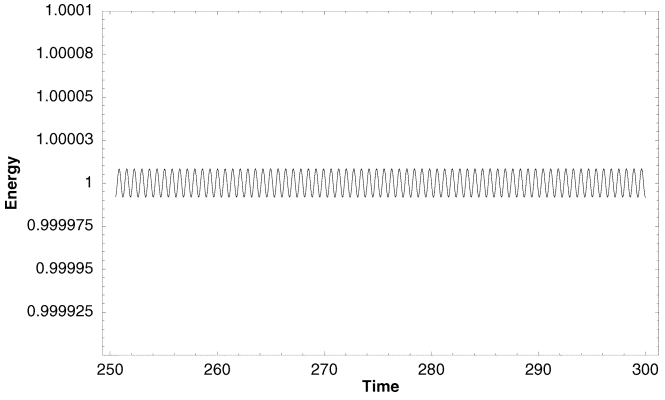

Fig. 6. Numerical energy at each time step for the third-order method.

maximum global phase error two orders of magnitude smaller than the first-order method for roughly the same computational cost.

Figs. 5 and 6 show the computed value of the numerical energy from (3) at each time step for both the first and third-order methods (for visual clarity, only values for the last 50 s are shown). Note that for both cases the numerical energy oscillates around the exact value, but for the third-order case, the amplitude of this oscillation is several orders of magnitude smaller than for first-order method, again for roughly the same computational cost.

B. Example 2

In this example we compute the resonant modes of the cubic cavity subject to a PEC boundary condition using two different integration methods. We do this by creating an oscillating electromagnetic field inside the cavity by applying a time dependent current source to a random sampling of the interior degrees of freedom. The simple current source has a temporal profile equal to the second derivative of a Gaussian pulse. Setting the speed of light equal to unity, we let the simulation run for a physical time of 300 s, then Fourier transform the resulting field amplitude to obtain both the transverse electric and transverse magnetic resonant modes of the cavity [21]. The errors for the first five excited modes of the cavity are computed using both a first-order and a third-order symplectic integration method. The exact values and the computed Fourier spectrum for the case of the third-order method are shown in Fig. 7. The results for both calculations are summarized in Table II. Again, note that for roughly the same computational cost, the third order method gives results that are more accurate than the first order method. We know from eigenvalue computation of Example 1 that the high-order spatial discretization is capable of computing the

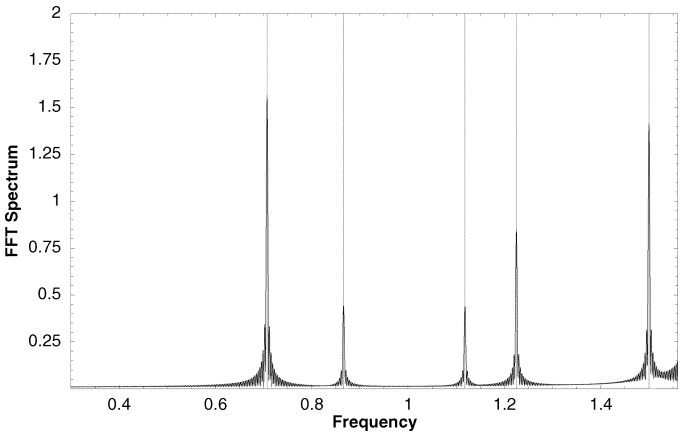

Fig. 7. Computed resonant modes of cubic cavity using a third order symplectic method. Vertical lines represent exact values.

TABLE II
COMPARISON OF RESULTS FOR TWO INTEGRATION METHODS

	1st Order	3rd Order
Physical Time	300 sec	300 sec
Time Step	0.005 sec	0.015 sec
No. Steps	60,000	20,000
Avg. CPU time/step	0.0941365 sec	0.297556 sec
Total Run Time	94.1 min	99.2 min
Error in 1st Mode	1.3809e-3	1.0935e-4
Error in 2nd Mode	8.9125e-4	3.8032e-4
Error in 3rd Mode	5.3780e-4	5.3780e-4
Error in 4th Mode	1.5442e-3	2.7264e-4
Error in 5th Mode	3.2044e-3	6.1035e-4

modes to an accuracy of 10^{-4}, and the data in Table II clearly shows this same accuracy can be achieved in the time domain only if a higher order time integration is used.

VI. CONCLUSION

The results of this paper are twofold. First, we have demonstrated that high-order time integration methods used in conjunction with high-order spatial discretizations can yield more accurate numerical results for roughly the same computational cost as a low-order method. Secondly, we have presented a general symplectic method for the integration of the time dependent Maxwell equations. Symplectic time integration methods have been developed for Hamiltonian systems such as those that arise in astrophysics and molecular dynamics, where very long time integration is required. We show that these methods can be successfully applied to a finite element discretization of Maxwell's equations, resulting in higher order and energy conserving integration. The higher order symplectic methods used in this paper are no more complicated or expensive than traditional Runge–Kutta methods.

REFERENCES

[1] J. M. Sanz-Serna and M. P. Calvo, *Numerical Hamiltonian Problems*. London, U.K.: Chapman and Hall, 1994.

[2] I. Saitoh, Y. Suzuki, and N. Takahashi, "The symplectic finite difference time domain method," *IEEE Trans. Magn.*, vol. 37, pp. 3251–3254, Sept. 2001.

[3] I. Saitoh and N. Takahashi, "Stability of symplectic finite-difference time-domain methods," *IEEE Trans. Magn.*, vol. 38, pp. 665–668, Mar. 2002.

[4] T. Hirono, W. W. Lui, and K. Yokoyama, "Time-domain simulation of electromagnetic field using a symplectic integrator," *IEEE Microwave Guided Wave Lett.*, vol. 7, no. 9, pp. 279–281, 1997.

[5] T. Hirono, W. W. Lui, K. Yokoyama, and S. Seki, "Stability and numerical dispersion of symplectic fourth-order time-domain schemes for optical field simulation," *J. Lightwave Tech.*, vol. 16, no. 10, pp. 1915–1920, 1998.
[6] O. C. Zienkiewicz, *The Finite Element Method in Engineering Science.*. London, UK.: McGraw-Hill, 1971.
[7] J. C. Nédélec, "Mixed finite elements in R3," *Numer. Math.*, vol. 35, pp. 315–341, 1980.
[8] D. A. White, "Numerical modeling of optical gradient traps using the vector finite element method," *J. Comput. Phys.*, vol. 159, no. 1, pp. 13–37, 2000.
[9] R. Rieben, D. White, and G. Rodrigue, "Improved conditioning of finite element matrices using new high-order interpolatory bases," *IEEE Trans. Antennas Propagat.*, 2004, to be published.
[10] J. Dao and J. Jin, "A general approach for the stability analysis of the time domain finite element method for electromagnetic simulations," *IEEE Trans. Antennas Propagat.*, vol. 50, pp. 1624–1632, Nov. 2002.
[11] G. Rodrigue and D. White, "A vector finite element time-domain method for solving Maxwell's equations on unstructured hexahedral grids," *SIAM J. Sci. Comp.*, vol. 23, no. 3, pp. 683–706, 2001.
[12] P. Thoma, "Numerical stability of finite difference time domian methods," *IEEE Trans. Magn.*, vol. 34, pp. 2740–2743, Sept. 1998.
[13] F. L. Teixeira and W. C. Chew, "Lattice electromagnetic theory from a topological viewpoint," *J. Math. Phys.*, vol. 40, no. 1, pp. 169–187, 1999.
[14] S. D. Gedney and J. A. Roden, "Numerical stability of nonorthogonal FDTD methods," *IEEE Trans. Antennas Propagat.*, vol. 48, pp. 231–239, Feb. 2000.
[15] D. Ruth, "A canonical integration technique," *IEEE Trans. Nucl. Sci.*, vol. NS-30, pp. 2669–2671, Aug. 1983.
[16] E. Forest and D. Ruth, "Fourth-order symplectic integration," *Physica D*, vol. 43, no. 1, pp. 105–117, 1990.
[17] A. M. Stewart and A. R. Humphries, *Dynamical Systems and Numerical Analysis*: Cambridge University Press, 1996.
[18] H. Yoshida, "Symplectic integrators for Hamiltonian-systems – Basic theory," in *Proc. IAU Symposia (152)*, The Netherlands, 1992, pp. 407–411.
[19] J. Candy and W. Rozmus, "A symplectic integration algorithm for seperable Hamiltonian functions," *J. Comput. Phys.*, vol. 92, pp. 230–256, 1991.
[20] D. A. White and J. M. Koning, "Computing solenoidal eigenmodes of the vector Helmholtz equation: A novel approach," *IEEE Trans. Magn.*, vol. 38, pp. 3420–3425, Sept. 2002.
[21] C. Balanis, *Advanced Engineering Electromagnetics*. New York: Wiley, 1989, vol. 75.